Application of Transient Aerodynamics to the Structural Nonlinear Flutter Problem

L. O. Brase*
McDonnell Aircraft Company, St. Louis, Missouri
and
W. Eversman†
University of Missouri—Rolla, Rolla, Missouri

A method is presented for the transient, time domain solution of the structural nonlinear flutter problem. Excellent agreement between the linear standard reduced frequency and transient flutter solutions is obtained for both a simplified two-degree-of-freedom system with Theodorsen two-dimensional incompressible unsteady aerodynamics and a multiple-degree-of-freedom system with three-dimensional compressible unsteady aerodynamics. The transient solution is then utilized to develop an approach for precisely including the effects of structural nonlinearities. This approach provides the capability of using the same detailed structural and aerodynamic models for both linear and nonlinear analyses.

Nomenclature

a = distance from midchord to elastic axis
$\bar{a}$ = complex aerodynamic stiffness load coefficient
b = reference semichord
b_o = reference semichord
$\bar{b}$ = complex aerodynamic damping load coefficient
d = distance from elastic axis to c.g.
e = base of natural logarithm
f = frequency, Hz
$f(t)$ = arbitrary input
$f(ik)$ = transfer function
g = structural damping
h = plunge coordinate
h = displacement normal to aerodynamic surface
$h(t)$ = unit impulse response
i = imaginary number
k = reduced frequency
k_h = plunge stiffness
k_m = Roger transfer function circulatory aerodynamic lag
k_α = pitch stiffness
m = mass
$m_{\nu\mu}$ = generalized mass matrix
p = Laplace operator
q = dynamic pressure
q = generalized coordinate
$r(t)$ = convolution integral
s = Laplace operator
t = real time
t' = real time
v = generalized velocity
x = generalized coordinate
z_m = Roger generalized aerodynamic lag
A_m = Roger aerodynamic transfer function constants
$A_{\nu\mu}$ = steady-state generalized aerodynamic stiffness matrix
$\bar{A}_{\nu\mu}$ = oscillatory complex generalized aerodynamic stiffness matrix
B = Roger dynamic matrix
$B_{\nu\mu}$ = steady-state generalized aerodynamic damping matrix
$\bar{B}_{\nu\mu}$ = oscillatory complex generalized aerodynamic damping matrix
C = structural damping
$C_{\nu\mu}$ = structural viscous damping matrix
$C_{h\alpha}$ = Theodorsen unsteady aerodynamic coefficient
$C(k)$ = aerodynamic transfer function
$C(\omega)$ = aerodynamic transfer function
$G_{\nu\mu}$ = generalized aerodynamic damping matrix (time-lagged component)
$H_{\nu\mu}$ = generalized aerodynamic damping matrix (instantaneous component)
$H(p)$ = Laplace transfer of system impulse response
$H(\omega)$ = Fourier transfer of system impulse response
I_α = pitch inertia
$I_{\nu\mu}$ = generalized aerodynamic inertia
$J_{\nu\mu}$ = generalized aerodynamic stiffness matrix (instantaneous component)
K = structural stiffness matrix
$K_{\nu\mu}$ = structural stiffness matrix
$L_{\nu\mu}$ = generalized aerodynamic stiffness matrix (time-lagged component)
$L.E.$ = leading edge
M = structural mass matrix
M = Theodorsen pitching moment
M = number of simple poles
$M^{\mu\nu}$ = inverse of combined structural and aerodynamic inertia matrix
N = number of aeroelastic generalized coordinates
P = Theodorsen aerodynamic plunging force
Q = aerodynamic force
Q_ν = total generalized aerodynamic force
$\bar{Q}_\nu$ = total complex oscillatory generalized aerodynamic force
$R(t)$ = steady-state response to unit harmonic input
S = area of aerodynamic surface
$S1B$ = stabilator first bending
V = airspeed
V_F = divergent flutter velocity
V_r = reference airspeed
α = pitch coordinate
α_0 = initial pitch rotation
$\alpha_{\nu\mu i}$ = time constants for aerodynamic stiffness transfer functions

Presented as Paper 87-0908 at the AIAA Dynamics Specialists Conference, Monterey, CA, April 9–10, 1987; received June 9, 1987; revision received Oct. 7, 1987.

*Senior Engineer, Technology–Structural Dynamics & Loads. Senior Member AIAA.
†Curator's Professor, Mechanical & Aerospace Engineering. Associate Fellow AIAA.

$\beta_{\nu\mu\iota}$ = time constants for aerodynamic damping transfer functions
ϵ = index for generalized coordinate
ι = index for state variables
μ = index for generalized coordinate
ν = index for generalized coordinate
π = 3.141593
ρ = air density
τ = dummy integrating variable
τ = transfer function time constants
ω = frequency, rad/sec
Λ^{ι} = convolution integral of generalized displacement
Ω^{ι} = convolution integral of generalized velocity

Introduction

ALTHOUGH nature is generally nonlinear, linearization has allowed the idealization of physical systems with simplified equations that are more easily solvable and for which the principle of superposition applies. Constant coefficient linear assumptions are adequate in most instances where all masses are constant and all spring and damping forces are proportional to the corresponding deflection and velocity component. However, experience has shown that phenomena exist that cannot be explained without addressing nonlinearity.

From an aircraft flutter perspective, nonlinearities can be either structural or aerodynamic, and categorically, either elastic or damping in nature. Structural nonlinearities can further be subdivided into distributed nonlinearities, which continue throughout the entire structure due to fastener elastodynamic deformations, and concentrated ones, which act locally as in control mechanisms or wing/external store connections.[1] Elastic examples include large amplitude oscillation and springs that exhibit hardening (friction), or softening (freeplay). Figure 1 illustrates representative restoring forces vs amplitude for a nominal linear spring and comparable springs with friction and freeplay. These nonlinearities exhibit a distinguishing characteristic in that the natural frequency is a function of the amplitude of oscillation. The method developed below addresses the concentrated, elastic, structural, nonlinear flutter problem.

Overview

The general flutter matrix equations of motion are

$$[M]\underline{\ddot{x}} + [K]\underline{x} = \underline{Q} \tag{1}$$

For the structural nonlinear problem, $[K]$ is not constant but a function of the system response amplitude. Solutions to second-order nonlinear differential equations are classified as either exact or approximate. An exact solution is defined in closed form or in an expression that can be numerically evaluated to any desired degree of accuracy. There are basically no exact solutions for nonlinear forced vibration except if the system can be described in a stepwise linear fashion. Such is the case for systems with hardening or softening springs; however, the use of transient aerodynamics, by definition an approximation of the forcing function, does not allow this proposed method to be entirely classified as an exact solution.

Approximate stability solutions are the most frequently used for aeroelastic studies. Although these do not yield a total solution in that the complete shape of the response motion is not determined, the solutions do indicate whether the system is stable or unstable. One of the best known and most extensively used stability methods is the "describing function"[2-4] or "harmonic balance"[5] method, a simplified version of the Kryloff and Bogoliuboff method.[6] This approach was first applied in the field of control system theory, an area in which the aeroelastician has recently become more familiar with the emergence of aeroservoelasticity as an important design and validation tool. The major assumption of this method is that the nonlinear system admits a periodic solution dominated by the fundamental harmonic. Thus, the effects from all higher harmonics are neglected. Miller[7] saw the potential of this technique as a design aid for tactical missile control surfaces, and Laurenson and Trn[8] applied it to a specific design with freeplay considerations. Describing functions were also used in the survey paper of Breitbach[1], as the theoretical correlation for a two-degree-of-freedom wind-tunnel test[9], and with an iterative procedure for multiple nonlinearities.[10]

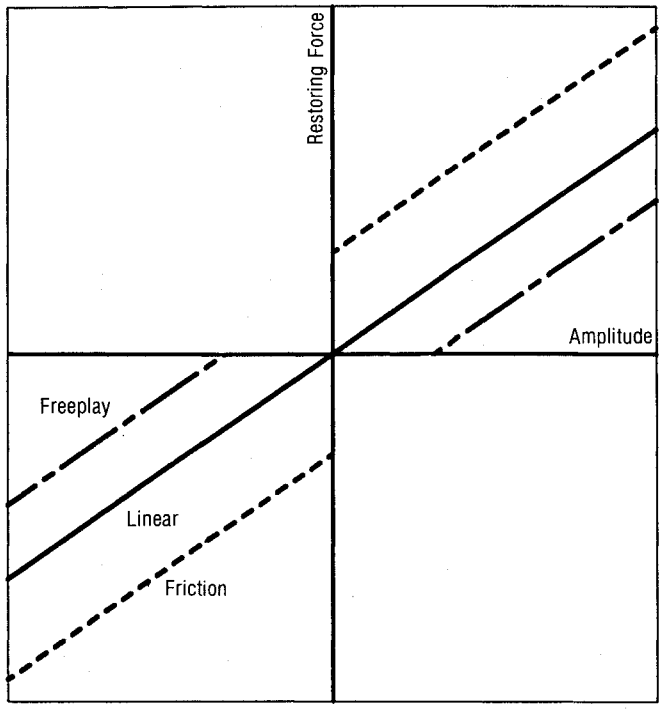

Fig. 1 Typical spring stiffnesses.

The analytical procedures described above approximate the nonlinear system by "equivalent" linearizations. These studies used simplified structural and/or aerodynamic modeling techniques, and, therefore, they can best be described as preliminary design tools. Thus, there is a definite need for a much more accurate analytical technique capable of coupling the detailed structural and aerodynamic equations of motion typical of current linear flutter methods used for final design verification. Where this was once thought to be an unnecessary and burdensome task, recent developments associated with today's lightweight/highly maneuverable aircraft, plus advancements in computer capabilities, have lent new credence to this endeavor. The purpose of the following studies is to outline a thorough yet general approach to the structural nonlinear flutter problem.

Theoretical Development

An essential ingredient of the nonlinear solution is the use of transient aerodynamics. The derivation of transient aerodynamics is based upon harmonic motion theory such as is traditionally used in the standard reduced frequency flutter solution. The equations of motion are derived for the standard solution by assuming that instability is defined as sustained zero-damped harmonic oscillation. Therefore, the exact flutter point is the only solution of physical significance. The use of subcritical ($g < 0$) or supercritical ($g > 0$) results to predict the onset of flutter is theoretically incorrect. The transient flutter solution, derived for arbitrary motion instead of simple harmonic motion, eliminates this discrepancy. Compared to the traditional Fourier transform approach, the

transient Laplace transform problem seems complicated. However, since the derived equations of motion are linear, superposition theory is as valid in the time domain as it is in the frequency domain. The application of Aseltine's method[11] to the flutter problem demonstrates that arbitrary motion in the time domain is accomplished by superposition of two elementary solutions, namely, response to unit impulse and to unit step inputs.

Using the following four relationships, the arbitrary transient response method is developed directly from the harmonic motion approach under the assumptions that the system is casual, i.e., can have no output until there is an input, and is stable. The steady-state response to a unit harmonic input is given by

$$R(t) = H(\omega)e^{i\omega t} \tag{2}$$

where $H(\omega)$ is the Fourier transform of the system impulse response. The unit impulse response is therefore defined as

$$h(t) = \frac{1}{2\pi}\int_{-\infty}^{\infty} H(\omega)e^{i\omega t}\,d\omega \tag{3}$$

the inverse Fourier transform of the transfer function $H(\omega)$. Known as the convolution integral,

$$r(t) = \int_0^t f(\tau)h(t-\tau)\,d\tau \tag{4}$$

presents the system response to an arbitrary input $f(t)$ as a function of the unit impulse response. Finally,

$$\begin{aligned} H(\omega) &= \int_0^{\infty} h(t)e^{-i\omega t}\,dt = H(p)/p = i\omega \\ &= \int_0^{\infty} h(t)e^{-pt}\,dt/p = i\omega \end{aligned} \tag{5}$$

the Fourier transform is the Laplace transform $H(p)$ evaluated on $p = i\omega$. The condition of causality $h(t) = 0$ for $t < 0$ guarantees that $h(t)$ vanishes for time less than zero so that the Fourier transform integration is defined only for positive time. Since the stability condition means the integral from zero to infinity of $|h(t)|$ is bounded, the requirement that the Fourier transform be absolutely integrable is satisfied. The inverse Fourier transform converts the function to the time domain for implementation of time history simulation. Further conversion, by the Laplace transform, yields a form compatible with transient response stability analysis. The approximate transfer function $H(\omega)$ is formulated so the Laplace transform is readily generated.

For harmonic motion, the generalized aerodynamic forces in the frequency domain are

$$\underline{Q}(t) = q[C(\omega)]\underline{x}_o e^{i\omega t} = q[C(k)]\underline{x}_o e^{i\omega t} \tag{6}$$

where $\underline{Q}(t)$ is the response or output, $q[C(\omega)]$ or $q[C(k)]$ is the transfer function, and $\underline{x}_o e^{i\omega t}$ is the input. The transfer function, a product of the dynamic pressure and the unsteady aerodynamic coefficient matrix, is dependent on frequency or reduced frequency, and each matrix element is a unique transfer function. Since the unsteady aerodynamic coefficients are normally not known as continuous functions of frequency ω, but rather at discrete values of reduced frequency k, an approximate transfer function is used to develop the continuous function necessary for transient analysis. The Roger[12] and Burkhart[13] procedures will be respectively utilized for Theodorsen[14,15] two-dimensional incompressible and doublet lattice[16] three-dimensional compressible unsteady aerodynamic theories. These are the two procedures that appear to have the most potential. Therefore, through familiarization, the best of these can be chosen for additional studies.

Applications

The general procedure will first be demonstrated on the simplest form of flutter, a two-dimensional airfoil section allowed to move with only two degrees-of-freedom (D.O.F.). These two motions represent the fundamental bending or torsion of the lifting surface and are commonly referred to as plunging and pitching, respectively. The standard linear reduced frequency system equations of motion are

$$\begin{bmatrix} m & m\,d \\ m\,d & m\,d^2 + I_\alpha \end{bmatrix}\begin{Bmatrix} \ddot{h} \\ \ddot{\alpha} \end{Bmatrix} + \begin{bmatrix} k_h & 0 \\ 0 & k_\alpha \end{bmatrix}\begin{Bmatrix} h \\ \alpha \end{Bmatrix} = \begin{Bmatrix} P \\ M \end{Bmatrix} \tag{7}$$

$$\begin{Bmatrix} P \\ M \end{Bmatrix} = q\begin{bmatrix} C_{hh} & C_{h\alpha} \\ C_{\alpha h} & C_{\alpha\alpha} \end{bmatrix}\begin{Bmatrix} h_0 \\ \alpha_0 \end{Bmatrix} e^{i\omega t} \tag{8}$$

The example used is the suspension bridge problem found in Fung.[17]

Roger's Approximate Unsteady Aerodynamic Transfer Function

Roger and Abel[18] suggested that the unsteady aerodynamic transfer function could be approximated by combining a second-order polynomial with a finite series of simple poles as

$$[C(k)] = [A_1] + [A_2](ik) + [A_3](ik)^2 + \sum_{m=4}^{M+3} \frac{[A_m](ik)}{(ik) + k_m} \tag{9}$$

where A_1 is the noncirculatory static-aerodynamics, A_2 (ik) is the aerodynamic damping, A_3 $(ik)^2$ is the apparent mass, and

$$\sum_{m=4}^{M+3} \frac{A_m(ik)}{(ik) + k_m}$$

are circulatory aerodynamic lags. The value of M can be 1, 2, 3, or 4, depending on the required accuracy. The k_m values are based on the best obtainable fit of the Theordorsen function. All the coefficients A_m are computed by the least-squares error method for a number of reduced frequencies at which the transfer function is defined.

By transforming the above into the Laplace domain,

$$[C(p)] = [A_1] + [A_2]\left(\frac{b}{V}\right)p + [A_3]\left(\frac{b}{V}\right)^2 p^2 + \sum_{m=4}^{M+3} \frac{[A_m]p}{p + p_m} \tag{10}$$

where

$$p_m = (V/b)k_m$$

The inverse Laplace transform yields

$$\begin{aligned} [C(t)] = {} & [A_1]\delta(t) + [A_2]\left(\frac{b}{V}\right)\dot{\delta}(t) + [A_3]\left(\frac{b}{V}\right)^2\ddot{\delta}(t) \\ & + \sum_{m=4}^{M+3} [A_m]\{\delta(t) - p_m e^{-p_m t}\} \end{aligned} \tag{11}$$

Since $[H(\omega)] = q[C(\omega)]$, then $[h(t)] = q[C(t)]$ defines the unit impulse response matrix as

$$\begin{aligned} [h(t)] = {} & q\left[\{[A_1] + \sum_{m=4}^{M+3} [A_m]\}\delta(t) + [A_2]\left(\frac{b}{V}\right)\dot{\delta}(t)\right. \\ & \left. + [A_3]\left(\frac{b}{V}\right)^2\ddot{\delta}(t) - \sum_{m=4}^{M+3} [A_m]p_m e^{-p_m t}\right] \end{aligned} \tag{12}$$

The definition of the convolution integral and introduction of a new variable

$$\underline{z}_m = \int_0^t \underline{x}(\tau)e^{-p_m(t-\tau)}\,d\tau \tag{13}$$

gives

$$\underline{Q}(t) = q([A_1] + \sum_{m=4}^{M+3} [A_m])\underline{x}(t) + q[A_2]\left(\frac{b}{V}\right)\underline{\dot{x}}(t) + q[A_3]\left(\frac{b}{V}\right)^2\underline{\ddot{x}}(t) - q\sum_{m=4}^{M+3}[A_m]p_m\underline{z}_m \tag{14}$$

Let

$$[\bar{A}_1] = [A_1] + \sum_{m=4}^{M+3}[A_m] \tag{15}$$

and substitute Eq. (14) into the general flutter equations of motion to obtain

$$([M] - q\left(\frac{b}{V}\right)^2[A_3])\underline{\ddot{x}} + ([C] - q\left(\frac{b}{V}\right)[A_2])\underline{\dot{x}} + ([K] - q[\bar{A}_1])\underline{x} + q\sum_{m=4}^{M+3}[A_m]p_m\underline{z}_m = \underline{0} \tag{16}$$

Substitution of the following:

$$\underline{\dot{x}} = v \tag{17a}$$

$$\underline{\ddot{x}} = \dot{v} \tag{17b}$$

$$[\hat{M}] = [M] - q\left(\frac{b}{V}\right)^2[A_3] \tag{17c}$$

$$[\hat{C}] = [C] - q\left(\frac{b}{V}\right)[A_2] \tag{17d}$$

$$[\hat{K}] = [K] - q[\bar{A}_1] \tag{17e}$$

$$[\hat{A}_m] = qp_m[A_m] \tag{17f}$$

and rearrangement simplifies to

$$[\hat{M}]\underline{\dot{v}} = -[\hat{C}]\underline{v} - [\hat{K}]\underline{x} - \sum_{m=4}^{M+3}[\hat{A}_m]\underline{z}_m \tag{18}$$

Differentiation of Eq. (13) gives

$$\underline{\dot{z}}_m(t) = \underline{x}(t) - p_m\underline{z}_m(t) \tag{19}$$

with

$$\underline{z}_m(0) = \underline{0}$$

The combination of Eqs. (18) and (19) with the definition $\underline{\dot{x}} = \underline{v}$, provides a new set of first order differential equations. Since this form is rather cumbersome, it will be represented symbolically as

$$\underline{\dot{v}} = [B]\underline{v} \tag{21}$$

The solution of the transient linear eigenvalue problem will produce (2 + M) times N eigenvalues λ and eigenvectors v_o, where M is the number of simple poles in Roger's approximate unsteady aerodynamic transfer function, and N is the number of modal degrees of freedom.

Time History Response Solution

Direct integration of Eq. (20) yields a time history response solution that could be used for a more thorough comparison with experimental data. As will be demonstrated in the following section, this type of solution is necessary to introduce structural nonlinearities into the system equations of motion.

The Advanced Continuous Simulation Language (ACSL)[19] was utilized since it was developed expressly for the purpose of modeling, on a digital computer, systems described by time-dependent, nonlinear differential equations and/or transfer functions. A fourth-order Runge-Kutta algorithm was chosen for the integration.

From the transient solution, linear eigenvalue stability and time history response analyses were performed for one-four simple poles.[20] The zero damped flutter results were within 1% of the standard solution for all cases. These two solutions differ primarily in damping, but the transient solution provides the more accurate theoretical prediction of subcritical or supercritical damping.

Nonlinear Transient Flutter

Unlike linear flutter, nonlinear flutter is highly dependent upon initial conditions. To limit the number of analyses, freeplay was chosen as the representative structural nonlinearity to demonstrate the methodology. The freeplay was also limited to the pitch D.O.F. for the spring stiffness variation, and the initial conditions were only allowed in pitch rotation. Modification of the time history procedure incorporated the nonlinearity into the equations of motion such that the amplitude dependent pitch spring stiffness k varied. Three separate freeplay bands, all symmetric about the origin, were analyzed.[20]

Time histories are provided by Fig. 2 for the ± 0.2 deg freeplay and 0.1 deg initial pitch rotation condition. Velocity was varied from 0 to 190 ft/s. At zero velocity, the plunge responds at its natural frequency of 0.14 Hz while the initial rotation, well within the freeplay region, is not enough to excite any pitch movement. Increasing the velocity to 17 ft/s applies enough aerodynamic force to generate a 0.07 Hz pitch oscillation, a subharmonic of the plunge response. Note that the dashed line will typically indicate the freeplay region. A doubling of velocity shows both D.O.F. vibrating at 0.14 Hz, and the plunge amplitude is experiencing a beating amplitude variation. Both modes are responding at their respective natural frequencies at 50 ft/s. The pitch rotation has now moved outside the positive freeplay band. This trend continues until both modes begin to move at approximately 0.20 Hz from 117 to 150 ft/s. Whereas the linear system fluttered at

$$\begin{Bmatrix} \underline{\dot{v}} \\ \underline{\dot{x}} \\ \underline{\dot{z}}_4 \\ \vdots \\ \underline{\dot{z}}_{M+3} \end{Bmatrix} = \begin{bmatrix} -[\hat{M}]^{-1}[\hat{C}] & -[\hat{M}]^{-1}[\hat{K}] & -[\hat{M}]^{-1}[\hat{A}_4] & \cdots & -[\hat{M}]^{-1}[\hat{A}_{M+3}] \\ [I] & [0] & [0] & \cdots & [0] \\ [0] & [I] & -p_4[I] & [0] & [0] \\ \vdots & \vdots & [0] & \ddots & [0] \\ [0] & [I] & [0] & [0] & -p_{M+3}[I] \end{bmatrix} \begin{Bmatrix} \underline{v} \\ \underline{x} \\ \underline{z}_4 \\ \vdots \\ \underline{z}_{M+3} \end{Bmatrix} \tag{20}$$

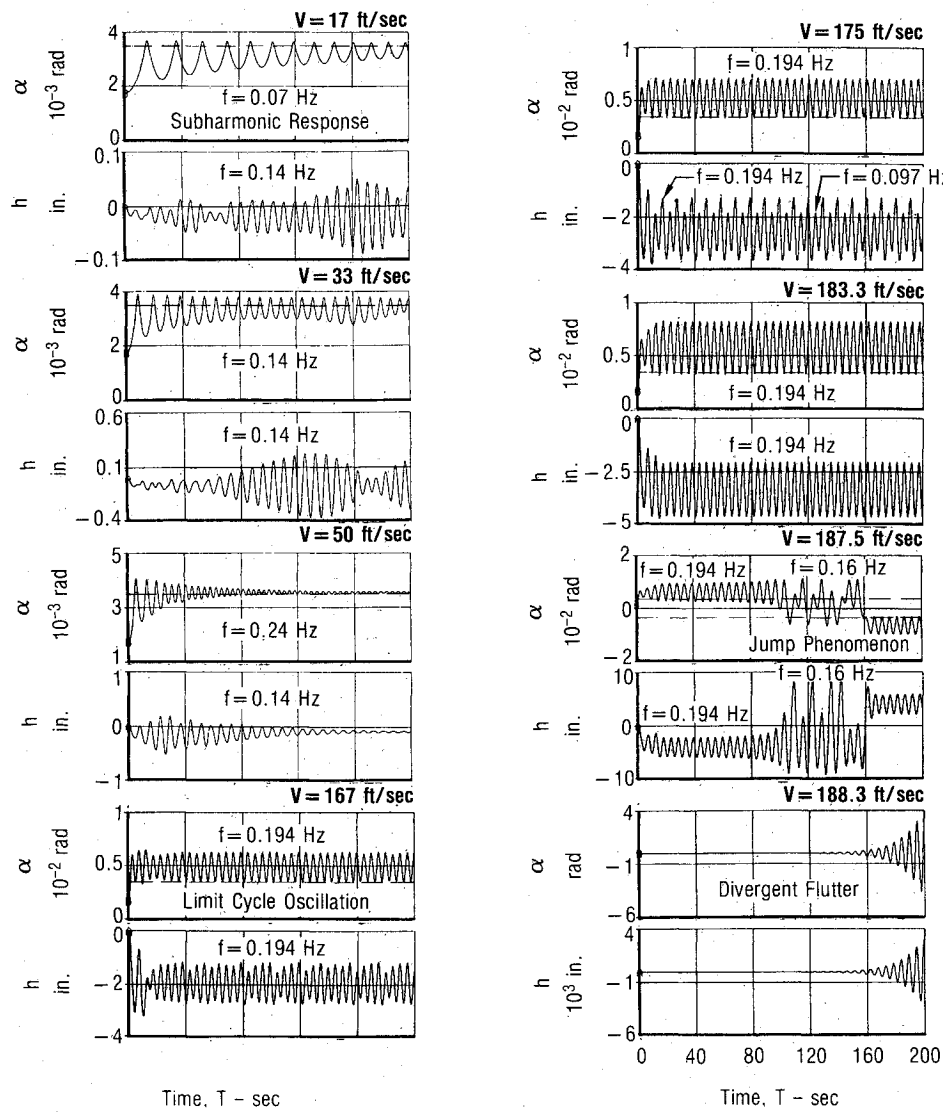

Fig. 2 Nonlinear two D.O.F. transient flutter; freeplay = ±0.2 deg; one simple pole; α_0 = 0.1 deg.

approximately 160 ft/s and 0.20 Hz, the nonlinear system develops into a small amplitude limit cycle oscillation. The limit cycle continues at 175 ft/s with an increase in amplitude. Also, the plunge displacement exhibits a distinct subharmonic 0.097 Hz frequency component. Both traces are clearly responding only at 0.194 Hz for 183.3 ft/s, and the amplitude has again increased. At 187.5 ft/s, a jump phenomenon occurs. The pitch rotation, which had been oscillating above the positive freeplay band, undergoes what appears as the onset of divergence response and jumps across the freeplay region to oscillate below the negative freeplay band. Similarly, the plunge displacement, which had been moving with solely negative deflection, jumps across to purely positive vibration. The motion amplitude decreases back to the previous magnitude. Note that the jump is not instantaneous, but it requires a few cycles before settling at the new steady-state vibration amplitude. Finally, divergent oscillation occurs at 188.3 ft/s, approximately 26 ft/s above the linear flutter velocity.

Even though a limit cycle oscillation was encountered at essentially the same velocity as the linear system, the amplitude and frequency were low enough that damage should be negligible. Therefore, for this particular case, a ±0.2 deg freeplay and 0.1 deg initial pitch rotation, the nonlinearity effectively raises the flutter speed. Two other bands of freeplay, ±1 deg and ±5 deg, were also analyzed, as presented in Fig. 3. Since the limit cycle oscillation is a steady-state constant amplitude "stable" condition, and response amplitude and frequency are low, the flutter velocity will be defined as the onset of divergent oscillation. The results indicate a similar trend as the initial pitch rotation angle is increased from 0.1 deg (within the freeplay band) to 20 deg (outside the freeplay band). The flutter speed increased above the corresponding linear case to approximately 190 ft/s. It remained essentially constant until, at some critical initial rotation well outside the particular freeplay region, the flutter velocity abruptly dropped below the linear case to about 155 ft/s. From thereon, the flutter speed asymptotically increased to the linear flutter speed.

Multiple-Degree-of-Freedom Three-Dimensional Flutter

Although two-dimensional theory is very useful in understanding the basic nature of flutter, it is inadequate for an accurate detailed analysis because of the assumptions that the aerodynamic flow is incompressible, and the system has an infinite aspect ratio. No spanwise variation of mass, stiffness, geometry, force, or response is considered. Therefore, a thorough flutter assessment requires the use of a multiple-degree-of-freedom, three-dimensional theory.

The stabilator of an F/A-18 Hornet was selected to demonstrate the methodology. Analytical results were substantiated by ground vibration tests, wind-tunnel tests, and flight tests. For these studies, the root support was slightly simplified such that the root was cantilevered except for the inclusion of the actuator pitch rotational stiffness. The stabilator was modeled by a structural elastic axis theory, or lumped-mass beam-rod analogy, using the NASTRAN[21] structural analysis program.

The three-dimensional compressible unsteady aerodynamic forces were defined by the doublet lattice method.[16] The generalized force derivatives for loads due to the μth coordinate doing work on the νth coordinate are

$$\bar{Q}_{\nu\mu} = \rho V^2 \iint \left[\left(\frac{\partial \bar{a}}{\partial q^\mu} \right) + ik \left(\frac{\partial \bar{b}}{\partial q^\mu} \right) \right] \left(\frac{\partial h}{\partial q^\nu} \right) dS \tag{22}$$

and the nondimensional generalized force derivatives are computed by

$$R_{\nu\mu} + iI_{\nu\mu} = \frac{-1}{\pi k^2 b_o^2} \bar{Q}_{\nu\mu} \tag{23}$$

Burkhart's Approximate Unsteady Aerodynamic Transfer Function

The formulation of the approximate unsteady aerodynamic transfer function selected by Burkhart was

$$f = \frac{1 + \tau_1 ik + \tau_2 (ik)^2}{1 + |\tau_3| ik} \tag{24}$$

This satisfies the following requirements:

1) It goes to a value of one as k goes to zero.

2) It is the minimum order transfer function capable of satisfactorily approximating the complex variation of a typical aerodynamic force element with reduced frequency.

3) It can be transformed readily to a time or Laplace operator formulation.

4) It represents a stable system by requiring τ_3 to be positive. The last requirement alleviates numerical instability, but it created considerable difficulty in the selection of the procedure for evaluating the time constants τ. For instance, the constraint eliminates the use of a least-squares curve fit. A gradient cost function optimization algorithm proved to be the most dependable for this particular application, although it is a rather unsophisticated optimization procedure.

After algebraic expansion of the transfer function, transformation to dimensional frequency, and application of the inverse Fourier transform, the aerodynamic forces can be expressed using real-time integrals and derivatives of the generalized coordinates as

$$\begin{aligned} Q_\nu = {} & \rho I_{\nu\mu} \ddot{q}^\mu + \rho V H_{\nu\mu} \dot{q}^\mu + \rho V^2 J_{\nu\mu} q^\mu \\ & + \rho V^2 G_{\nu\mu} \int_0^t \dot{q}^\mu \exp\left(-\frac{V}{b_o} \frac{t - t'}{\beta_{\nu\mu 3}} \right) dt' \\ & + \rho V^3 L_{\nu\mu} \int_0^t q^\mu \exp\left(-\frac{V}{b_o} \frac{t - t'}{\alpha_{\nu\mu 3}} \right) dt' \end{aligned} \tag{25}$$

where

$$I_{\nu\mu} = b_o^2 B_{\nu\mu} \frac{\beta_{\nu\mu 2}}{\beta_{\nu\mu 3}}$$

$$H_{\nu\mu} = b_o \left[A_{\nu\mu} \frac{\alpha_{\nu\mu 2}}{\alpha_{\nu\mu 3}} + B_{\nu\mu} \left(\frac{\beta_{\nu\mu 1}}{\beta_{\nu\mu 3}} - \frac{\beta_{\nu\mu 2}}{\beta_{\nu\mu 3}^2} \right) \right]$$

$$J_{\nu\mu} = A_{\nu\mu} \left(\frac{\alpha_{\nu\mu 1}}{\alpha_{\nu\mu 3}} - \frac{\alpha_{\nu\mu 2}}{\alpha_{\nu\mu 3}^2} \right)$$

$$G_{\nu\mu} = B_{\nu\mu} \left(\frac{1}{\beta_{\nu\mu 3}} - \frac{\beta_{\nu\mu 1}}{\beta_{\nu\mu 3}^2} + \frac{\beta_{\nu\mu 3}}{\beta_{\nu\mu 3}^3} \right)$$

$$L_{\nu\mu} = \frac{A_{\nu\mu}}{b_o} \left(\frac{1}{\alpha_{\nu\mu 3}} - \frac{\alpha_{\nu\mu 1}}{\alpha_{\nu\mu 3}^2} + \frac{\alpha_{\nu\mu 2}}{\alpha_{\nu\mu 3}^3} \right)$$

The I matrix is analogous to aerodynamic inertia. The H and J matrices determine aerodynamic damping and stiffness forces. The G and L matrices determine aerodynamic damping and stiffness forces that have a time lag relative to the generalized velocities and displacements, respectively.

Eigenvalue Stability Solution

The incorporation of Eq. (25) into the general flutter equations of motion gives

$$\begin{aligned} & (m_{\nu\mu} - \rho I_{\nu\mu}) \ddot{q}^\mu + (C_{\nu\mu} - \rho V H_{\nu\mu}) \dot{q}^\mu \\ & + (K_{\nu\mu} - \rho V^2 J_{\nu\mu}) q^\mu - \rho V^2 G_{\nu\mu} \int_0^t \dot{q}^\mu \exp\left(-\frac{V}{b_o} \frac{t - t'}{\beta_{\nu\mu 3}} \right) dt' \\ & - \rho V^3 L_{\nu\mu} \int_0^t q^\mu \exp\left(-\frac{V}{b_o} \frac{t - t'}{\beta_{\nu\mu 3}} \right) dt' = 0 \end{aligned} \tag{26}$$

where $m_{\nu\mu}$ is the structural inertia matrix, $c_{\nu\mu}$ is the structural viscous damping, and $K_{\nu\mu}$ is the structural stiffness matrix.

The convolution integrals of Eq. (26) are formulated by introducing a set of state variables

$$\Lambda^\iota = \int_0^t q^\mu \exp\left(-\frac{V}{b_o} \frac{t - t'}{\alpha_{\nu\mu 3}} \right) dt' \tag{27a}$$

$$\Omega^\iota = \int_0^t \dot{q}^\mu \exp\left(-\frac{V}{b_o} \frac{t - t'}{\beta_{\nu\mu 3}} \right) dt' \tag{27b}$$

where the index $\iota = \nu + N(\mu - 1)$. In differential form

$$\dot{\Lambda}^\iota = q^\mu - \left(\frac{V}{b_o \alpha_{\nu\mu 3}} \right) \Lambda^\iota \tag{28a}$$

$$\dot{\Omega}^\iota = \dot{q}^\mu - \left(\frac{V}{b_o \beta_{\nu\mu 3}} \right) \Omega^\iota \tag{28b}$$

The lagged aerodynamic stiffness and damping matrices are reorganized to $N \times N^2$ size by

$$L_{\nu\iota} = L_{\nu\mu} \text{ and } G_{\nu\iota} = G_{\nu\mu} \text{ if } \iota = \nu + N(\mu - 1) \tag{29a}$$

$$L_{\nu\iota} = 0 \text{ and } G_{\nu\iota} = 0 \text{ if } \iota \neq \nu + N(\mu - 1) \tag{29b}$$

The form of the flutter equations of motion is now

$$\begin{aligned} \ddot{q}^\epsilon = {} & -M^{\mu\nu} [(C_{\nu\mu} - \rho V H_{\nu\mu}) \dot{q}^\mu + (K_{\nu\mu} - \rho V^2 J_{\nu\mu}) q^\mu \\ & - \rho V^2 G_{\nu\iota} \Omega^\iota - \rho V^3 L_{\nu\iota} \Lambda^\iota] \end{aligned} \tag{30}$$

where

$$[M^{\mu\nu}] = [m_{\nu\mu} - \rho I_{\nu\mu}]^{-1}$$

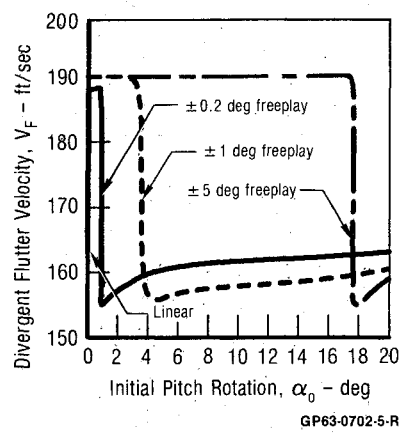

Fig. 3 Nonlinear two D.O.F. transient flutter; onset of divergent oscillation.

and the indices range as

$$\epsilon,\ \nu,\ \mu = 1,2,\ldots,\ N;\ l = 1,2,\ldots,\ N^2$$

If all of the initial conditions of the generalized coordinates are zero, the Laplace transforms of Eqs. (28) and (30) are

$$(m_{\nu\mu} - \rho I_{\nu\mu})s^2 q^\mu (C_{\nu\mu} - \rho V H_{\nu\mu}) s q^\mu + (K_{\nu\mu} - \rho V^2 J_{\nu\mu}) q^\mu - \rho V^2 G_{\nu l}\Omega^l - \rho V^3 L_{\nu l}\Lambda^l = 0$$

$$s\Lambda^\iota + \left(\frac{V}{b_o \alpha_{\nu\mu 3}}\right)\Lambda^\iota - q^\mu = 0$$

$$s\Omega^\iota + \left(\frac{V}{b_o \beta_{\nu\mu 3}}\right)\Omega^\iota - s q^\mu = 0$$

or

$$s\begin{Bmatrix}\Lambda\\ \Omega\\ q\\ sq\end{Bmatrix} = \left[\begin{array}{c|c|c|c} -(V/b_o\alpha_3) & 0 & \{1\}\ \{1\}\ \{1\}\ \ddots\ \{1\} & 0 \\ \hline 0 & -(V/b_o\beta_3) & 0 & \{1\}\ \{1\}\ \{1\}\ \ddots\ \{1\} \\ \hline 0 & 0 & 0 & 1\ 1\ 1\ \ddots\ 1 \\ \hline \rho V^3 ML & \rho V^2 MG & M[-K+\rho V^2 J] & M[-C+\rho V H] \end{array}\right] \begin{Bmatrix}\Lambda\\ \Omega\\ q\\ sq\end{Bmatrix} \tag{31}$$

The number of eigenvalues is $2(N^2 + N)$. Of these values, there are $2N$ roots that are complex conjugate pairs that represent the aeroelastic configuration. The other $2N^2$ roots are latent aerodynamic roots associated with the feedback state variables. These are always stable and either real or complex with a small imaginary magnitude.

Inertially Coupled Solution

The analyses presented in the previous section utilized the coupled normal modes approach to the solution. Although this is ideal for most linear flutter because of the associated reduction in problem size, it is undesirable for the structural nonlinear problem because of the complexity in determining whether or not the displacement dependent solution is inside or outside the influence of the nonlinearity.

Since the two D.O.F. problem consists of rigid modes, the generalized coordinate is either pure pitch or plunge by definition. However, the generalized coordinates of a flexible surface are modal D.O.F. such that the particular motion at any given spanwise position is not easily definable. Therefore, it is necessary to inertially couple rigid modes for D.O.F. that include nonlinearities, together with the basic flexible normal modes of the structure. For the stabilator, a rigid pitch rotation mode was inertially coupled to the first seven flexible cantilevered normal modes. The validity of this procedure is verified by the results provided in Fig. 4. Only minor differences are shown by the comparison with the transient analyses from the previous section.

Again, the damping predicted by the standard solution is only theoretically correct at $g = 0$, the flutter point. Therefore, the differences shown are expected. Analyses comparing transient and the standard reduced frequency flutter solutions were performed throughout the subsonic Mach range.[20] Both solutions used eight normal modes, although the figure only displays the first three modes. These results conclude that excellent agreement was achieved.

Time History Response Solution

Equation (30), the flutter equations of motion, and Eq. (28), the time lags from the growth of the aerodynamic loads, are of the form necessary for use in a time history response solution. The ACSL dynamic simulation language will again be utilized to directly integrate the differential equations.

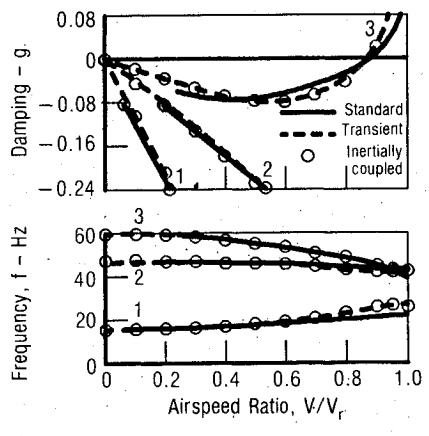

Fig. 4 Comparison of normal mode flutter with inertially coupled flutter; Mach 0.7.

The linear time history response solution for the inertially coupled stabilator is provided in Fig. 5. Once again, eight D.O.F. were used in the analyses. This equates to 144 transient equations of motion. Mode 1, first bending, and mode 8, pitch rotation, are presented for a selection of velocity ratios ranging from 0.86 to 0.90. An initial pitch rotation of 1 deg was used to excite the system. High frequency content was present in the reponse traces at the lower velocities. This indicates the participation of all modes in the response. As the velocity increases toward the instability, the traces "clean up" until only the 46 Hz motion is present at flutter.

Due to the size of the problem, the analyses were performed for a minimum number of airspeed ratios. However, linear interpolation verified that the onset of flutter occurs at the same ratio as predicted by the eigenvalue solution.

Nonlinear Transient Flutter

As was previously stated, nonlinear flutter is highly dependent upon the initial conditions. Since the size of the multiple D.O.F. problem has grown substantially larger than the two D.O.F. problem, the number of analyses was limited to a demonstration of the procedure.

Freeplay was again chosen to represent the structural nonlinearity. Similar to the two D.O.F. problem, both the freeplay and initial conditions were limited to the pitch rotation. The nonlinear spring stiffness k_α included a symmetric ± 1.0 deg dead band about the origin. Three cases were analyzed by varying the initial pitch rotation as 0.5, 1.5, and 10 deg. The latter case is presented as Fig. 6.

For velocity ratios less than 0.6, all oscillatory motion in the pitch rotation is suppressed by the freeplay. The response was highly damped until approximately $V/V_r = 0.85$, where the damping definitely began to decrease. Damping continued to decrease with increasing velocity until a 43 Hz limit cycle oscillation developed at $V/V_r = 0.9$. At this point, the amplitude of the pitch rotation motion was at the limit of the ± 1.0 deg freeplay region. A 0.01 increase in velocity ratio yielded little change except that the S1B displacement exhibited a slight beating in amplitude. The only noticeable difference in response from the airspeed ratio of 0.92 to 0.93 was a little increase in amplitude. Divergent oscillation occurred

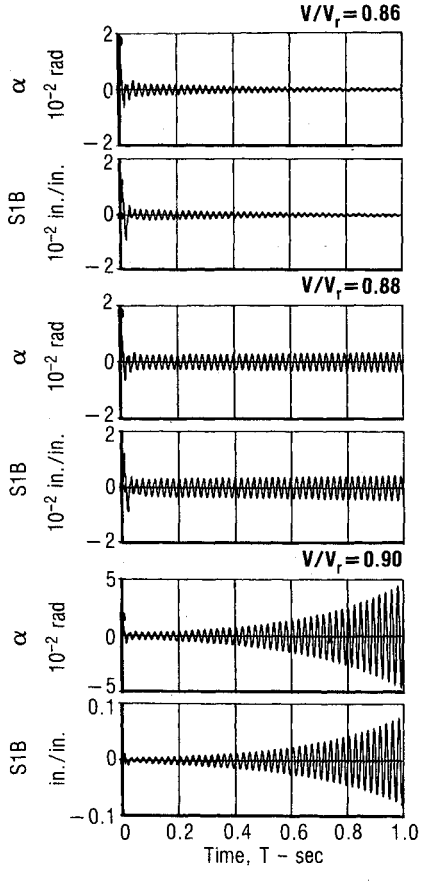

Fig. 5 Linear eight D.O.F. inertially coupled transient flutter; Mach 0.7, $\alpha_o = 10$ deg.

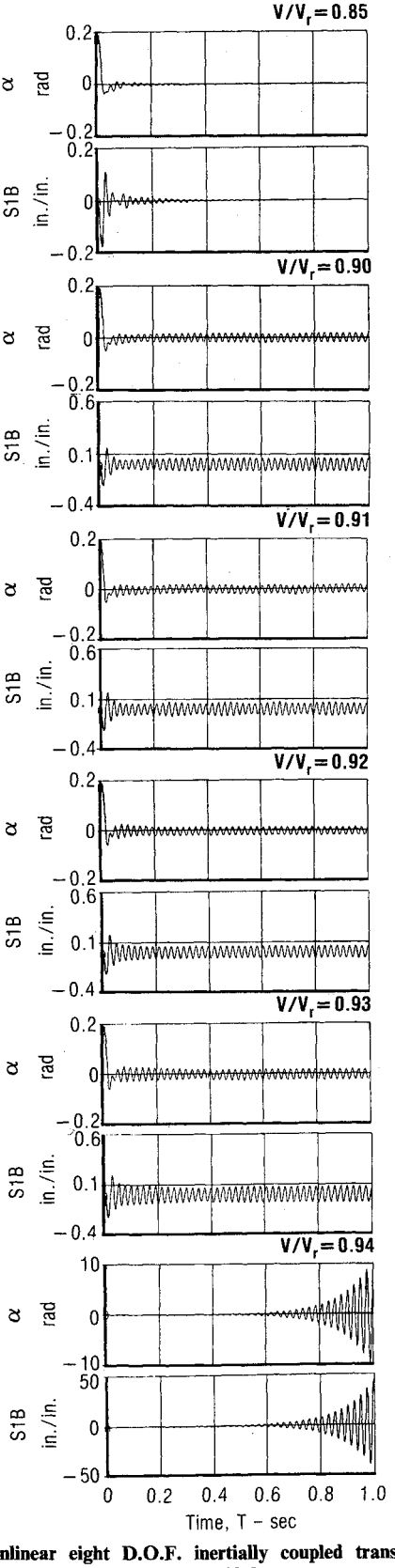

Fig. 6 Nonlinear eight D.O.F. inertially coupled transient flutter; freeplay = ± 1.0 deg; Mach 0.7, $\alpha_o = 10$ deg.

	Freeplay Band (deg)	Initial Pitch Rotation (deg)	Airspeed Ratio
Linear	—	Not Dependent	0.87
Nonlinear	±1.0	0.5	0.89 – 0.90
Nonlinear	±1.0	1.5	0.89 – 0.90
Nonlinear	±1.0	10	0.93 – 0.94

Fig. 7 Comparison of linear and nonlinear eight D.O.F. inertially coupled transient flutter; Mach 0.7.

between 0.93 and 0.94 as compared to 0.87 for the linear case. Figure 7 summarizes the flutter results for the three initial conditions. Although these results are not adequate to totally define the nature of this particular instability, there is some indication of a trend similar to that shown in Fig. 3 for the two D.O.F. problem. Those results showed that for a particular freeplay band, the flutter speed initially increased above the linear case with increasing initial pitch rotation amplitude. This increase in flutter speed continued until a point was reached where the flutter speed fell below and then asymptotically reapproached the linear result with continued increase in initial condition amplitude.

Conclusion

A precise solution method has been developed and demonstrated for the structural nonlinear flutter problem. The inclusion of three-dimensional compressible unsteady aerodynamics provides the capability of using the same detailed structural and aerodynamic models for both linear and nonlinear analyses. This solution has many advantages over a stability solution, but the disadvantage is the growth in problem size attributed to the transient aerodynamics. Where this was once a major drawback, the advancements in computational capability have not only made the solution of large problems feasible, but also practical.

Excellent agreement was obtained for both the two D.O.F. and multiple D.O.F. linear systems that were provided for familiarization and verification purposes. Thus, the inclusion of structural nonlinearities into the system equations of motion is theoretically correct. Although all results were presented for subsonic flight conditions, the procedure is equally valid for supersonic aerodynamic theories, since the transient solution calculates the aerodynamic transfer functions from harmonic generalized aerodynamic forces. The technique can be applied to any structural nonlinearity that can be represented in a stepwise linear fashion. This includes freeplay, friction, preload, and large amplitude stiffness variations. All of these effects can be considered alone or in combinations.

The Roger and Burkhart procedures, two different but similar formulations of the transient aerodynamic transfer function, were utilized. These were the two procedures that appeared to have the most potential. Based on the studies performed thus far, no conclusive preference could be justified. One advantage of the Roger formulation is problem size. For an N D.O.F. problem, Roger's method translates into $(2+M)(N)$ equations of motion (M being the number of simple poles), whereas Burkhart's method equates into $2(N^2+N)$ equations of motion. Obviously, the best approach would be the one that provides the required accuracy and the smallest problem size.

Since the nonlinear solution, which is dependent upon initial conditions, is typically a variation of the linear solution, which is independent upon initial conditions, knowledge of the latter proves very helpful. The flutter results of the two and eight D.O.F. nonlinear problems showed similar trends. Both developed the classic limit cycle oscillation instability prior to experiencing divergent flutter. Also, with increasing initial pitch rotation amplitude, the nonlinear flutter velocity initially increased above the linear flutter velocity. This increase in flutter speed continued until a critical initial condition was reached where the flutter speed fell below, and then asymptotically reapproached the linear result with further increase of initial condition amplitude.

References

[1]Breitbach, E., "Effects of Structural Non-Linearities on Aircraft Vibration and Flutter," AGARD Rept. 665, Sept. 1977.

[2]Greif, H. D., "Describing Function Method of Servomechanism Analysis Applied to Most Commonly Encountered Nonlinearities," *AIEE Transactions—Pt. II*, No. 8, Sept. 1953, pp. 243–248.

[3]Kochenburger, R. J., "A Frequency Response Method of Analyzing and Synthesizing Contactor Servomechanisms," *AIEE Transactions*, Vol. 69, Pt. I, 1950, pp. 270–284.

[4]Truxal, J. G., *Automatic Feedback Control System Synthesis*, McGraw-Hill, New York, 1955, Chap. 10.

[5]Shen, S. F., "An Approximate Analysis of Nonlinear Flutter Problems," *Journal of the Aero/Space Sciences*, Vol. 26, Jan. 1959, pp. 25–32, 45.

[6]Kryloff, N. and Bogoliuboff, N., *Introduction to Nonlinear Mechanics* (a free translation by S. Lefschetz), Princeton Univ. Press, Princeton, NJ, 1947.

[7]Miller, M. Z., "Two Degree of Freedom Flutter Analysis Including Effects of Structural Nonlinearities," McDonnell Douglas Astronautics Corp., St. Louis, MO, E236-ATN-001, Dec. 1972.

[8]Laurenson, R. M. and Trn, R. M., "Flutter of Control Surfaces with Structural Nonlinearities," *AIAA Journal*, Vol. 18, Oct. 1980, pp. 1245–1251.

[9]McIntosh, S. C., Jr., Reed, R. E., Jr., and Rodden, W. P., "An Experimental and Theoretical Study of Nonlinear Flutter," *Journal of Aircraft*, Vol. 18, Dec. 1981, pp. 1057–1063.

[10]Lee, C. L., "An Iterative Procedure for Nonlinear Flutter Analysis," *AIAA Journal*, Vol. 24, May 1986, pp. 833–840.

[11]Aseltine, J. A., *Transform Method in Linear System Analysis*, McGraw-Hill, New York, 1958.

[12]Roger, K. L., "Airplane Math Modeling Methods for Active Control Design," AGARD Rept. 228, April 1977.

[13]Burkhart, T. H., "Subsonic Transient Lifting Surface Aerodynamics," *Journal of Aircraft*, Jan. 1977, pp. 44–50.

[14]Theodorsen, T., "General Theory of Aerodynamic Instability and the Mechanism of Flutter," NACA TR-496, 1934.

[15]Theodorsen, T. and Garrick, I. E., "Mechanism of Flutter, a Theoretical and Experimental Investigation of the Flutter Problem," NACA TR–685, 1940.

[16]Kalman, T. P., Rodden, W. P., and Giesing, J. P., "Aerodynamic Influence Coefficients by the Doublet Lattice Method for Interfering Non-Planar Lifting Surfaces Oscillating in a Subsonic Flow," Douglas Aircraft Rept. DAC 67977, 1969.

[17]Fung, Y. C., *An Introduction to the Theory of Aeroelasticity*, Wiley, New York, 1955.

[18]Abel, I., "An Analytical Technique for Predicting the Characteristics of a Flexible Wing Equipped with an Active Flutter Suppression System and Comparison with Wind Tunnel Data," NASA TP 1367, Feb. 1979.

[19]Mitchell and Gauthier Assoc., Inc., *Advanced Continuous Simulation Language (ACSL) User Guide/Reference Manual*, Mitchell and Gauthier Assoc., Inc., Concord, MA, 1981.

[20]Brase, L. O., "The Application of Transient Aerodynamics to the Structural Nonlinear Flutter Problem," Thesis Univ. of Missouri—Rolla, Rolla, MO, July 1986.

[21]MacNeal, R. H., "The NASTRAN Theoretical Manual," NASA SP–221(01), Dec. 1973.